Involvement of neutrophils in machineries underlying the rupture of intracranial aneurysms

Mika Kushamae
  National Cerebral and Cardiovascular Center

Haruka Miyata
  Shiga University of Medical Science

Manabu Shirai
  National Cerebral and Cardiovascular Center

Kampei Shimizu
  Kyoto University Graduate School of Medicine

Mieko Oka
  Tokyo Women's Medical University

Hirokazu Koseki
  Jikei University School of Medicine

Yu Abekura
  Kyoto University Graduate School of Medicine

Isao Ono
  Kyoto University Graduate School of Medicine

Kazuhiko Nozaki
  Shiga University of Medical Science

Tohru Mizutani
  Showa University

Tomohiro Aoki (✉ tomoaoki@ncvc.go.jp)
  National Cerebral and Cardiovascular Center

Research

Abstract

Background: Subarachnoid hemorrhage due to rupture of an intracranial aneurysm (IA) has quite a poor prognosis once after the onset despite of the modern technical advancement. The development of a novel therapeutic modality to prevent rupture or a diagnostic method to stratify dangerous lesions from many stable ones is thus mandatory for social health. To this end, mechanisms underlying rupture of lesions should be clarified.

Methods: We and others have developed the rat model in which induced IAs spontaneously rupture resulting in subarachnoid hemorrhage. To clarify molecular cascades regulating rupture, we obtained gene expression profile data from rupture-prone lesions and revealed the enrichment of neutrophil-related terms in rupture-prone lesions by Gene Ontology analysis. Next, to validate a role of neutrophils in rupture of lesions, G-CSF was administered to a rat model.

Results: As a result, G-CSF treatment not only increased number of neutrophils infiltrating in lesions but also significantly facilitated rupture of the lesions without increase the incidence. To clarify mechanisms how neutrophils facilitate rupture of IAs, we used HL-60 cell line and found that inflammatory stimuli enhanced the collagenolytic activity of MMP9. Immunohistochemical study using IA lesions from a rat model identified neutrophils as a major type of cells producing MMP9 around a site of rupture and consistently the collagenolytic activity of MMP9 was detected in ruptured lesions.

Conclusions: These results combined together suggest the crucial role of neutrophil to rupture of IAs and also propose the potential of this type of cells as a candidate of therapeutic or diagnostic targets.

Background

The rupture of intracranial aneurysms (IAs) accounts for 85% of spontaneous subarachnoid hemorrhage (SAH) [1]. The incidence of SAH is 9.1/100,000 people per year in a population-based study but remarkable regional variation is present [1]. It is well-recognized that the incidence is higher in Finnish (19.7/100,000 people per year) and Japanese (22.7/100,000 people per year) [1]. SAH has a considerable negative impact on a society due to its high mortality or morbidity. SAH occasionally causes the sudden death even in a young people, e.g. 8.3% of affected persons die at a site of the onset without subjecting to the medical care [2]. Also even if patients suffered from SAH are successfully given the treatment, 29.7% of them experiences the severe morbidity (modified Rankin Scale > 2) and 12.1% is dead [2].

Considering above devastating outcome of SAH once after the onset, a development of a novel therapeutic strategy based on the correct understanding of machineries underlying rupture of IAs is mandatory for social health. The rat model of IAs in which induced lesions spontaneously and frequently rupture resulting in SAH has recently been reported [3, 4]. As histopathological examinations of this model have revealed the close similarity with human IAs; e.g. remarkable degenerative changes in media, infiltrating of inflammatory cells or loss of endothelial cells [5–7], a similar machinery regulating rupture of lesions presumably functions also in this rat model. We thus in this study examined differences in the

comprehensive gene expression profile data between rupture-prone IA lesions and the remaining arterial walls in the circle of Willis to explore differentially represented cascades as a candidate mediating rupture of the lesion.

Methods

IA models of rats and histological analysis of induced IA

All of the following experiments, including animal care and use, complied with the National Institute of Health's Guide for the Care and Use of Laboratory Animals and complied with the National Institute of Health's Guide for the Care and Use of Laboratory Animals and were approved by the Institutional Animal Care and Use Committee of National Cerebral and Cardiovascular Center. The present manuscript adheres to the ARRIVE (Animal Research: Reporting of In Vivo Experiments) guidelines for reporting animal experiments.

10-week-old female Sprague – Dawley (SD) rats were purchased from Japan SLC (Slc:SD, n = 69, Shizuoka, Japan). Animals were maintained on a light/dark cycle of 12 h/12 h, and had a free access to chow and water. To induce IAs, rats were subjected to the bilateral ovariectomy, the ligation of the left carotid artery, the right external carotid artery and the right pterygopalatine artery, and systemic hypertension achieved by the combination of a high salt diet and the ligation of the left renal artery [4] under general anesthesia by the combination of intraperitoneal injection of pentobarbital sodium (50 mg/kg) with inhalation of Isoflurane (1.5 ~ 2%). Immediately after surgical manipulations, animals were fed the chow containing 8% sodium chloride and 0.12% 3-aminopropionitrile (Tokyo Chemical Industry, Tokyo, Japan), an irreversible inhibitor of Lysyl Oxidase catalyzing the cross-linking of collagen and elastin. Dead animals within one week after surgical manipulations were excluded from the analyses. At 8 weeks in RNA sequencing analysis or 9 weeks in histopathological examination after above surgical manipulations, animals were deeply anesthetized by intraperitoneal injection of pentobarbital sodium (200 mg/kg), and transcardially perfused with 4% paraformaldehyde solution. The circle of Willis was then stripped from brain surface and an IA lesion induced at an anterior communicating artery or a posterior communicating artery was dissected as a rupture-prone lesion if SAH was macroscopically not detected. All dead animals during the observation period were autopsied to examine the onset of SAH. If SAH was observed, the ruptured IA lesions were stripped and histopathologically examined. Histopathological examination was done after Elastica van Gieson staining or Azan staining.

G-CSF treatment

G-CSF (300 ∝g/kg, MOCHIDA PHARMACEUTICAL CO., LTD., Tokyo, Japan) was subcutaneously administered to rats twice a week from the 28th day to the 56th day after surgical manipulations. The number of myeloperoxidase (MPO)-positive cells or CD68-positive cells was calculated as a cell count

present within 1 mm square around the dome of induced IAs. The dose of G-CSF administered in rats were determined by the preliminary dose-response analyses.

RNA purification and RNA sequencing analysis

Dissected rupture-prone aneurysms and the remaining circle of Willis from a same animal were grinded and homogenized in liquid nitrogen. Total RNA was isolated from homogenized samples with a RNeasy fibrous tissue mini kit (QIAGEN, Hilden, Germany) with an on-column DNase treatment, according to manufacturer's instructions. Quantity of each total RNA sample was measured with a NanoDrop (Thermofisher, Waltham, MA), and its quality was assessed by using the RNA integrity number (RIN) on an Agilent 4200 Tapestation (Agilent, Santa Clara, CA). The libraries from purified RNA samples (500 ng) for RNA sequencing analyses were then prepared using a TruSeq stranded mRNA sample preparation kit (Illumina, San Diego, CA). Paired-end sequencing (2 × 75 base pair) was performed on a NextSeq500 (Illumina). Each read was then mapped to the Rattus norvegicus reference genome (Rnor6) by CLC genomics workbench (version 11, QIAGEN). Differential expression analyses including principal component analysis and gene ontology (GO) analysis were performed using the RNA-Seq tool, one similar to the DESeq and the edgeR package, in CLC genomics workbench. Genes whose expression reaches a fold change over 1.5 in aneurysm lesions compared with that in the remaining circle of Willis were considered as over- or under-expressed ones.

All the raw data from RNA sequencing analysis was deposited to Gene Expression Omnibus (https://www.ncbi.nlm.nih.gov/geo/) (ID # Data will be deposited after the acceptance.).

Immunohistochemistry

At the indicated period after the aneurysm induction, 5-um-thick frozen sections were prepared. After blocking with 3% donkey serum (Jackson ImmunoResearch, Baltimore, MD), slices were incubated with primary antibodies followed by incubation with secondary antibodies conjugated with a fluorescence dye (Jackson ImmunoResearch). Finally, fluorescent images were acquired on a confocal fluorescence microscope system (FV1000 or FV3000, Olympus, Tokyo, Japan).

The following primary antibodies were used: Cy3-conjugated mouse monoclonal anti-α-smooth muscle actin (SMA) antibody (#C6198, Sigma-Aldrich, St. Louis, MO), mouse monoclonal anti-rat CD68 antibody (#ab31630, Abcam, Cambridge, UK), rabbit polyclonal anti-MMP9 antibody (#ab38898, Abcam), rabbit polyclonal anti-myeloperoxidase (MPO) antibody (#ab9535, Abcam), rabbit polyclonal anti-GRO alpha (CXCL-1) antibody (#ab86436, Abcam) and rabbit polyclonal anti-Histone H3 (citrulline R2 + R8 + R17) antibody (#ab5103, Abcam).

Cell line

HL-60 cell line used as a model of neutrophils was purchased from ATCC (#CCL-240, Manassas, VA) and maintained in Dulbecco's Modified Eagle's Medium (DMEM) supplemented with 20% fetal bovine serum (Sigma-Aldrich).

Quantitative real time (RT)-PCR analysis in cultured cells

HL-60 cells were stimulated with recombinant TNF-α (100 ng/ml, R&D SYSTEMS, Minneapolis, MN) for 90 min. Total RNA was then purified from stimulated cells and reverse-transcribed by using a RNeasy Mini Kit (QIAGEN) and a High-capacity cDNA Reverse Transcription Kit (Life Technologies Corporation, Carlsbad, CA) according to the manufacturers' instructions. For quantification of gene expression, RT-PCR was performed on a Real Time System CFX96 (Bio-rad, Hercules, CA) using a SYBR Premix Ex Taq II (TAKARA BIO INC., Shiga, Japan). Expression of ACTB was used as the internal control. For quantitation, the second derivative maximum method was used for determining the crossing point.

Primer sets used are listed in Additional file 1.

Gelatin Zymography

HL-60 cells were stimulated with recombinant TNF-α (100 ng/ml) for 90 min. The supernatant was then prepared and collagenolytic activity in the supernatant was examined by a gelatin zymography as the manufacture's instructions (Gelatin Zymography Kit, Cosmo Bio Co., LTD., Tokyo, Japan). In a rat model, ruptured IA lesions were harvested and grinded in a liquid nitrogen. Specimens were then lysed and subjected to a gelatin zymography as the manufacture's instructions (Gelatin Zymography Kit, Cosmo Bio Co., LTD.).

The concentration of TNF-α or PGE $_2$ in the culture supernatant

HL-60 cells were stimulated with recombinant TNF-α (100 ng/ml) or LPS (10 ∝g/ ml, SIGMA, Lot # 123M4052V) for 5 h. In some experiments, cells were pre-treated with indomethacin for 15 min (100 nM, Wako). The supernatant was then prepared and the concentration of TNF-α or PGE_2 in the supernatant was examined as the manufacture's instructions (Quantikine ELISA for human TNF-α, R&D SYSTEMS, or Prostaglandin E_2 EIA Kit, Cayman Chemical, Ann Arbor, MI).

Statistical analysis

Data are shown by box-and-whisker plots. Statistical comparisons between 2 groups were conducted using a Mann – Whitney U test and comparisons among more than 2 groups were done by a Kruskal –

Wallis test followed by a Steel test. The incidence of IAs or SAH was analyzed by a Fisher's exact test. A p value smaller than 0.05 was defined as statistically significant.

Results

Up-representation of cascades related with neutrophils in RNA sequencing analysis

15 rats were subjected to the surgical manipulations to induce IAs [4] and, at 9 weeks after manipulations, 5 out of them developed IAs at the anterior- or posterior communicating artery; among them, one was ruptured and other 4 were unruptured lesions. From these 4 rats with unruptured IAs, the circle of Willis was stripped and unruptured lesions at the anterior- or posterior communicating artery were harvested as a rupture-prone lesion (Additional file 2: fig. S1). Total RNA samples purified from dissected IA tissues and the remaining circle of Willis were then subjected to RNA sequencing analyses to obtain gene expression profile data and to identify cascades specifically up-represented in rupture-prone IA lesions compared with that in the remaining circle of Willis. RNA samples from one IA specimen and the corresponding remaining circle of Willis were excluded from the analysis with the corresponding circle of Willis because of the low RNA yield. The median value of RIN of RNA samples used in RNA sequencing analyses was 7.9 and 8.1 (n = 6). Reads mapped in pairs obtained in the present experiment was between 161 and 176 million. Among these reads, 88.1% of fragments per sample on average were successfully mapped to the reference rat genome (Rnor6). Principal component analysis demonstrated variability among the rupture-prone IA samples, suggesting the heterogeneity of the lesions (Fig. 1a). Considering the heterogeneity of the lesions (Fig. 1a) and the findings that more than half of rupture-prone lesions will rupture [4], we picked up genes whose expression was over-expressed in all the IA samples in common compared with that in the remaining circle of Willis. We then identified a couple of differentially expressing genes, 568 over-expressed and 961 under-expressed ones, in rupture-prone IAs compared with those in the remaining arterial walls in the circle of Willis (Fig. 1b and 1c, Additional file 3 and 4). Through GO analysis using 568 over-expressed genes by CLC genomics workbench system, 228 terms were picked up as up-represented ones in IA lesions. Intriguingly, these terms contained several neutrophil- or leukocyte-related ones (Fig. 1d), suggesting the role of neutrophils in the process regulating the rupture of lesions. In the heat map, individual variabilities were observed as is the case with principal component analysis (Fig. 1a). Genes over-expressed in rupture-prone IAs included ones coding some chemoattractants for inflammatory cells like Ccl2 and Ccl3, Ccl6, Ccl7 and cytokines like Il1b (Fig. 1e). Because some of these factors play a role in the pathogenesis of IAs [8–10], the contribution of neutrophils to the pathogenesis of IAs in terms of inflammation is further supported.

Accumulation of neutrophils around the site of rupture in IA lesions

We next examined whether neutrophils indeed could be detected in IA lesions especially ruptured ones in immunohistochemistry for a marker of neutrophils, MPO. In immunohistochemical examination of ruptured IA lesions from a rat model, the accumulation of MPO-positive cells, neutrophils, was observed almost strictly around the site of rupture although those cells could be rarely detected in other part of aneurysmal walls (Fig. 2). Note that there were some vasa vasorum with a SMA-positive medial smooth muscle cell layer specifically around the site of rupture and neutrophils accumulated nearby (Fig. 2), suggesting the infiltration of neutrophils through vasa vasorum. Here, we have recently clarified the association of the induction of vasa vasorum formation with rupture of IAs presumably via facilitating the infiltration of inflammatory cells [4]. These results combined together indicate that the accumulation of neutrophils through vasa vasorum induced exacerbates inflammatory responses at the prospective site of rupture and resultant degenerative changes of arterial walls in situ leading to rupture of IAs. In this sense, we hypothesized that machineries mediating rupture of lesions was driven only in the tiny area in IA walls.

Effect of increase in number of neutrophils in lesions on the rupture of IAs

To corroborate the contribution of neutrophils and neutrophil-mediated machineries on the rupture of IAs, G-CSF was administered to a rat model to increase the number of neutrophils infiltrating in lesions (Fig. 3a). 300 ∝g/kg G-CSF administered in a model indeed increased the number of neutrophils infiltrating in IA lesions over 20 folds and the differences reached statistically significant (Fig. 3b and 3c). 21 rats were subjected to IA induction; 14 rats out of them were treated with G-CSF (300 ∝g/kg, twice/week, s.c.) and remaining 7 rats were allocated to the vehicle-treated group. 8 aneurysms in 14 G-CSF-treated rats (57.1%) or 3 aneurysms in 7 vehicle-treated rats (42.9%) were induced at the anterior- or posterior communicating artery. G-CSF treatment thus did not influence the incidence of IAs (Fig. 3d). Importantly, the incidence of SAH in G-CSF-treated rats (7/14 rats, 50%; 7/8 aneurysms, 87.5%) was significantly higher than that in the vehicle-treated group (0/7 rats; 0/3 aneurysms) (Fig. 3e and 3f). In immunohistochemistry, most MPO-positive neutrophils were positive for citrullinated histone H3 (Cit-H3) (Fig. 4a), a marker of the neutrophil extracellular traps, indicating the activation [11, 12] presumably due to cytokines present in the microenvironment. Consistently, most positive signals for MPO in immunohistochemistry was also positive for CXCL-1 (Fig. 4b), a cytokine with chemotactic activity for neutrophils [13, 14], suggesting the formation of auto-amplification loop among themselves to accumulate in situ as observed in the present experiment (Fig. 2) as in macrophages in IAs [7]. Although neutrophils was accumulated and activated in IA walls specifically around the site of rupture, the number of infiltrated macrophages, a cell type significantly contributing to the formation and progression of the disease [8, 9, 15, 16], in whole lesions was not different between G-CSF-treated and vehicle-treated groups (Additional file 2: fig.S2). Considered with the findings that neutrophils accumulated specifically at the tiny area in IA lesions (Fig. 2) but could facilitate rupture (Fig. 3), neutrophils might function to facilitate the degenerative changes of arterial walls in the microenvironment only around a site of rupture.

Contribution of neutrophils to rupture of IAs

In AZAN staining of ruptured IA lesions, destructive changes in connective tissues were most remarkable just around the site of rupture (Fig. 5a). Thereby, we next examined whether neutrophils could directly degenerate the extracellular matrix mainly collagens using HL-60 cells. The gelatin zymography to detect the collagenolytic activity revealed the presence of the collagenase activity in the supernatant of cultured neutrophils and the activity was presumably derived from MMP2 and MMP9 referencing the recombinant MMP2 and MMP9 served as a control (Fig. 5b and Additional file 2: fig. S3). Note that no other bands than MMP2 and MMP9 were visible in the gel (Additional file 2: fig. S3). Importantly, the collagenase activity of MMP9 was remarkably enhanced under the inflammatory stimuli by TNF-α which is present in IA lesions and contributes to the pathogenesis [17]. Consistently, mRNA expression of MMP9 was specifically among proteinases examined and significantly induced under the stimulation with TNF-α (Fig. 5c). We next examined whether neutrophils accumulating around the site of rupture produced MMP9 in vivo in immunohistochemistry. MMP9 expression was indeed detected in IA walls and most of the positive signals for MMP9 in immunostaining was co-localized with those for a marker of neutrophils, MPO (Fig. 5d). Importantly and consistently, the collagenolytic activity of MMP9 was detected in ruptured lesions (Fig. 5e), suggesting the in vivo relevance of above in vitro study. Also in neutrophils, the expression of pro-inflammatory genes, PTGS2, IL6 and TNF, was induced under the stimulation with TNF-α (Additional file 2: fig.S4a) and, consistently, the secretion of Prostaglandin E_2 and TNF-α in the culture supernatant was enhanced (Additional file 2: fig.S4b, 4c). These results combined together with the well-established concept that IA is the chronic inflammatory disease affecting intracranial arteries [7, 15, 18] suggest that neutrophils, not macrophages, actively participate in and rather trigger the molecular machineries leading to rupture of the lesions.

Discussion

In the present study, the contribution of neutrophils to the process leading to rupture of the lesions has been suggested. Because neutrophils infiltrating in lesions produce tissue-destructive proteinases like MMP9 (Fig. 5d), neutrophils accumulated in microenvironment can directly exacerbate the degenerative changes of atrial walls and presumably facilitate rupture of the lesions. In addition, as demonstrated in in vitro experiments (Additional file 2: fig. S4), neutrophils can produce a large amount of pro-inflammatory factors like TNF-α and PGE_2 in response to the cytokines present in situ to provide inflammatory microenvironment and to exacerbate inflammatory responses there presumably in concert with macrophages activated by neutrophil-producing cytokines. Immunohistochemical analyses also support the activation of neutrophils in lesions (Fig. 4a). Intriguingly, neutrophils in lesions produce CXCL-1 (Fig. 4b) and form the auto-amplification loop to accumulate in lesions leading to the formation of inflammatory microenvironment at the prospective site of rupture like macrophages in lesions [7, 16]. Considering the crucial contribution of TNF-α or PGE_2 in the pathogenesis of IAs [7, 19–21], neutrophils in addition to macrophages presumably play a pivotal role in the maintenance and exacerbation of inflammatory responses facilitating the degenerative changes in lesions. The involvement of

inflammatory responses in lesions in the process leading to rupture has also been supported by the observation studies that the usage of drugs with anti-inflammatory effects like statins and non-steroidal anti-inflammatory drugs reduces the risk of SAH due to rupture of IAs [22, 23]. Some studies about human IAs have also provided evidence indicating the association of neutrophils with the progression of IAs. For example, previous histopathological studies have suggested the infiltration of inflammatory cells including neutrophils in IA lesions [24, 25]. The histological study enrolling three ruptured and 20 unruptured IA specimens harvested during operation has demonstrated that all of the three ruptured lesions and half of the unruptured ones were positive for MPO staining in immunohistochemistry [26]. Importantly, MPO-positive group has a significantly higher risk of rupture within 5 years (2.28%) estimated by PHASES scoring system [27] than that in MPO-negative group (0.69%) [26], suggesting the involvement of neutrophil-mediated pathway in the process leading to rupture. In the other study, 36 saccular intracranial aneurysms, 16 unruptured and 20 ruptured lesions, were immuno-stained and positive signals for MPO were detected in all aneurysm lesions [28]. Because the extent of MPO-positive area in immunohistochemistry was significantly correlated with the degenerative changes in arterial walls of the lesions or infiltration of inflammatory cells including macrophages [28], the crucial contribution of MPO-positive neutrophils in the progression of the disease is again implicated. Intriguingly, the study enrolling 25 IA cases and examining the concentration of MPO in plasma from IA lesions and femoral artery has demonstrated the significant increase in the concentration of MPO in plasma from IA lesions compared with that from femoral artery, supporting the role of MPO or neutrophils in microenvironment of the lesions to progress the disease. Although the careful interpretation is necessary especially whether MPO activity indeed reflects the activity of neutrophils, the genetic deletion of MPO results in the suppression of SAH in mice model of IAs in which lesions are induced by the systemic hypertension and elastase infusion [29], providing the experimental evidence to suggest the contribution of neutrophils to rupture of IAs.

In the present study, through in vivo and in vitro studies, the crucial role of neutrophil-mediated machineries in rupture of IAs has been highlighted. Intriguingly, accumulating evidence mainly through experimental studies using animal models of IAs has revealed the involvement of macrophages and macrophage-mediated inflammatory responses in the pathogenesis of IAs, especially initiation and progression of the disease [7−9, 16, 18, 30]. Considering results from the present study and previous findings [7−9, 15], type of cells contributing in each process of the disease development may be different; macrophages in initiation and progression, neutrophils in rupture. In rat model of IAs, IA lesions were induced at an anterior cerebral-olfactory artery bifurcation in almost all animals investigated but these lesions never rupture. On the contrary, the incidence of lesions at an anterior communication artery or posterior communicating artery bifurcation was only 50% but these lesions have a high potential of rupture [4]. Combined these findings together, a different machinery may be involved in each step of the disease development and contributing type of cells is presumably different accordingly.

In the present study, we have identified the accumulation of neutrophils around the site of rupture and propose the crucial contribution of neutrophil-mediated tissue destruction and exacerbation of inflammation to rupture of the lesions. In this point of view, a non-invasive imaging of the presence or the

activation of this type of cells in lesions could be an ideal diagnostic method to more exactly predict rupture of lesions or stratify rupture-prone lesions from many stable ones. Nano-particle-based visualization of neutrophils in MRI as in macrophages [31–33] may have potential to become such a novel diagnostic method. Although the excellent specificity to neutrophils is essential as a diagnostic method to accurately reflect the presence or the activity of them, the specificity enough for a usage for a diagnosis still remains to be established.

Conclusions

This study using a rat model of IAs have suggested the crucial role of neutrophils in the process leading to rupture of IAs. In this process, this type of cells forms the self-amplification loop via CXCL-1 to form inflammatory environment and facilitates degenerative changes of arterial walls leading to rupture of the lesions via producing tissue-destructive proteinases like MMP9. Also, neutrophils could exacerbate inflammatory responses in situ through secreting cytokines. This study has thus proposed the potential of neutrophils as a candidate of therapeutic or diagnostic targets. Considered with the poor outcome of SAH and the resultant social loss due to the lack of medical therapy, the present study can greatly contribute not only to the field of vascular biology but also to the social health.

Declarations

Ethics approval and consent to participate

Animal studies including this manuscript was approved by the Institutional Animal Care and Use Committee of National Cerebral and Cardiovascular Center (Approval No. 17085, 18010, 19036).

Consent for publication

Not applicable.

Availability of data and materials

The datasets used and/or analysed during the current study are available from the corresponding author on reasonable request.

Competing interests

Funding

Author's contributions

M.K., H. M., M. S. and T. A. planned the experiments. M.K., H. M., M. S., K. S., M. O., H. K., Y. A., I. O. and T. A. acquired the data. M.K., H. M., M. S., K. S., M. O., H. K., Y. A., I. O., K. N., T. M. and T. A. interpreted the data. M.K., H. M., M. S. and T. A. wrote the manuscript. K. N., T. M. and T. A. critically reviewed and modified the manuscript. All authors read and approved the final manuscript.

Acknowledgements

Not applicable.

References

1. Macdonald RL, Schweizer TA. Spontaneous subarachnoid haemorrhage. Lancet. 2017;389(10069):655-66.

2. Nieuwkamp DJ, Setz LE, Algra A, Linn FH, de Rooij NK, Rinkel GJ. Changes in case fatality of aneurysmal subarachnoid haemorrhage over time, according to age, sex, and region: a meta-analysis. Lancet Neurol. 2009;8(7):635-42.

3. Miyamoto T, Kung DK, Kitazato KT, Yagi K, Shimada K, Tada Y et al. Site-specific elevation of interleukin-1beta and matrix metalloproteinase-9 in the Willis circle by hemodynamic changes is associated with rupture in a novel rat cerebral aneurysm model. J Cereb Blood Flow Metab. 2017;37(8):2795-805.

4. Miyata H, Imai H, Koseki H, Shimizu K, Abekura Y, Oka M et al. Vasa vasorum formation is associated with rupture of intracranial aneurysms. J Neurosurg. 2019:1-11.

5. Aoki T, Nishimura M. The development and the use of experimental animal models to study the underlying mechanisms of CA formation. J Biomed Biotechnol. 2011;2011:535921.

6. Hashimoto N, Handa H, Hazama F. Experimentally induced cerebral aneurysms in rats. Surg Neurol. 1978;10(1):3-8.

7. Aoki T, Frosen J, Fukuda M, Bando K, Shioi G, Tsuji K et al. Prostaglandin E2-EP2-NF-kappaB signaling in macrophages as a potential therapeutic target for intracranial aneurysms. Sci Signal. 2017;10(465).

8. Aoki T, Kataoka H, Ishibashi R, Nozaki K, Egashira K, Hashimoto N. Impact of monocyte chemoattractant protein-1 deficiency on cerebral aneurysm formation. Stroke. 2009;40(3):942-51.

9. Kanematsu Y, Kanematsu M, Kurihara C, Tada Y, Tsou TL, van Rooijen N et al. Critical roles of macrophages in the formation of intracranial aneurysm. Stroke. 2011;42(1):173-8.

10. Aoki T, Koseki H, Miyata H, Itoh M, Kawaji H, Takizawa K et al. RNA sequencing analysis revealed the induction of CCL3 expression in human intracranial aneurysms. Sci Rep. 2019;9(1):10387.

11. Meher AK, Spinosa M, Davis JP, Pope N, Laubach VE, Su G et al. Novel Role of IL (Interleukin)-1beta in Neutrophil Extracellular Trap Formation and Abdominal Aortic Aneurysms. Arterioscler Thromb Vasc Biol. 2018;38(4):843-53.

12. Warnatsch A, Ioannou M, Wang Q, Papayannopoulos V. Inflammation. Neutrophil extracellular traps license macrophages for cytokine production in atherosclerosis. Science. 2015;349(6245):316-20.

13. Moser B, Clark-Lewis I, Zwahlen R, Baggiolini M. Neutrophil-activating properties of the melanoma growth-stimulatory activity. J Exp Med. 1990;171(5):1797-802.

14. Schumacher C, Clark-Lewis I, Baggiolini M, Moser B. High- and low-affinity binding of GRO alpha and neutrophil-activating peptide 2 to interleukin 8 receptors on human neutrophils. Proc Natl Acad Sci U S A. 1992;89(21):10542-6.

15. Aoki T, Narumiya S. Prostaglandins and chronic inflammation. Trends Pharmacol Sci. 2012;33(6):304-11.

16. Aoki T, Yamamoto R, Narumiya S. Targeting macrophages to treat intracranial aneurysm. Oncotarget. 2017;8(62):104704-5.

17. Aoki T, Kataoka H, Morimoto M, Nozaki K, Hashimoto N. Macrophage-derived matrix metalloproteinase-2 and -9 promote the progression of cerebral aneurysms in rats. Stroke. 2007;38(1):162-9.

18. Shimizu K, Kushamae M, Mizutani T, Aoki T. Intracranial Aneurysm as a Macrophage-mediated Inflammatory Disease. Neurol Med Chir (Tokyo). 2019;59(4):126-32.

19. Aoki T, Fukuda M, Nishimura M, Nozaki K, Narumiya S. Critical role of TNF-alpha-TNFR1 signaling in intracranial aneurysm formation. Acta Neuropathol Commun. 2014;2:34.

20. Yokoi T, Isono T, Saitoh M, Yoshimura Y, Nozaki K. Suppression of cerebral aneurysm formation in rats by a tumor necrosis factor-alpha inhibitor. J Neurosurg. 2014;120(5):1193-200.

21. Starke RM, Chalouhi N, Jabbour PM, Tjoumakaris SI, Gonzalez LF, Rosenwasser RH et al. Critical role of TNF-alpha in cerebral aneurysm formation and progression to rupture. J Neuroinflammation. 2014;11:77.

22. Hasan DM, Mahaney KB, Brown RD, Jr., Meissner I, Piepgras DG, Huston J et al. Aspirin as a promising agent for decreasing incidence of cerebral aneurysm rupture. Stroke. 2011;42(11):3156-62.

23. Yoshimura Y, Murakami Y, Saitoh M, Yokoi T, Aoki T, Miura K et al. Statin use and risk of cerebral aneurysm rupture: a hospital-based case-control study in Japan. J Stroke Cerebrovasc Dis. 2014;23(2):343-8.

24. Kataoka K, Taneda M, Asai T, Kinoshita A, Ito M, Kuroda R. Structural fragility and inflammatory response of ruptured cerebral aneurysms. A comparative study between ruptured and unruptured cerebral aneurysms. Stroke. 1999;30(7):1396-401.

25. Frosen J, Piippo A, Paetau A, Kangasniemi M, Niemela M, Hernesniemi J et al. Remodeling of saccular cerebral artery aneurysm wall is associated with rupture: histological analysis of 24 unruptured and 42 ruptured cases. Stroke. 2004;35(10):2287-93.

26. Gounis MJ, Vedantham S, Weaver JP, Puri AS, Brooks CS, Wakhloo AK et al. Myeloperoxidase in human intracranial aneurysms: preliminary evidence. Stroke. 2014;45(5):1474-7.

27. Greving JP, Wermer MJ, Brown RD, Jr., Morita A, Juvela S, Yonekura M et al. Development of the PHASES score for prediction of risk of rupture of intracranial aneurysms: a pooled analysis of six prospective cohort studies. Lancet Neurol. 2014;13(1):59-66.

28. Ollikainen E, Tulamo R, Lehti S, Hernesniemi J, Niemela M, Kovanen PT et al. Myeloperoxidase Associates With Degenerative Remodeling and Rupture of the Saccular Intracranial Aneurysm Wall. J Neuropathol Exp Neurol. 2018;77(6):461-8.

29. Chu Y, Wilson K, Gu H, Wegman-Points L, Dooley SA, Pierce GL et al. Myeloperoxidase is increased in human cerebral aneurysms and increases formation and rupture of cerebral aneurysms in mice. Stroke. 2015;46(6):1651-6.

30. Aoki T. Inflammation mediates the pathogenesis of cerebral aneurysm and becomes therapeutic target. Neuroimmunology and Neuroinflammation. 2015;2(2):86.

31. Shimizu K, Kushamae M, Aoki T. Macrophage Imaging of Intracranial Aneurysms. Neurol Med Chir (Tokyo). 2019;59(7):257-63.

32. Hasan DM, Mahaney KB, Magnotta VA, Kung DK, Lawton MT, Hashimoto T et al. Macrophage imaging within human cerebral aneurysms wall using ferumoxytol-enhanced MRI: a pilot study. Arterioscler Thromb Vasc Biol. 2012;32(4):1032-8.

33. Aoki T, Saito M, Koseki H, Tsuji K, Tsuji A, Murata K et al. Macrophage Imaging of Cerebral Aneurysms with Ferumoxytol: an Exploratory Study in an Animal Model and in Patients. J Stroke Cerebrovasc Dis. 2017;26(10):2055-64.

Additional Materials

Additional file 1 (xls) Primer sets used in RT-PCR analyses.

Additional file 2 (PDF)

Fig.S1 IA lesion induced in a rat model

Rats were subjected to an IA model and the IA lesions including the surrounding the circle of Willis were harvested. The representative macroscopic image of the induced IA lesion (indicating by the dotted white circle) is shown. Bar; 1 mm.

Fig.S2 Influence of G-CSF treatment on the number of CD68-positive cells infiltrating in IA lesions of rats

IA lesions were harvested from rats subjected to an IA model and treated with G-CSF (300 µg/kg, G-CSF (+), n=14) or vehicle (G-CSF (-), n=7) as shown in Fig. 3a and immunostained. The cell count of CD68-

positive cells, macrophages, is shown. Data represents box-and-whisker plots. Statistical analysis was done by a Mann-Whitney *U* test.

Fig.S3 The collagenolytic activity in the supernatant of cultured neutrophils examined by a gelatin zymography

Cultured neutrophils (HL-60 cells) were stimulated with recombinant TNF-α (100 ng/ml, 5 h) and the collagenolytic activity in the supernatant was examined by a gelatin zymography using recombinant pro-MMP9 and MMP2 as a reference. The raw image of the gel used in Fig. 5b is shown.

Fig.S4 Production of pro-inflammatory factors from stimulated neutrophils

a Induction of pro-inflammatory genes by the stimulation with TNF-α in neutrophils. HL-60 cells used as neutrophils were stimulated with recombinant TNF-α (100 ng/ml, 90 min) and the expression of pro-inflammatory genes, *PTGS2* (which encodes COX-2), *IL6* and *TNF*, was examined in RT-PCR analysis (n=4). Data represents box-and-whisker plots. Statistical analysis was done by a Mann-Whitney *U* test. *; $p<0.05$. **b** and **c** Production of Prostaglandin E_2 or TNF-α from neutrophils under inflammatory stimuli. HL-60 cells were stimulated with recombinant TNF-α (100 ng/ml) or LPS (10 μg/ml) for 5 h and the supernatant was subjected to EIA or ELISA to measure the concentration of Prostaglandin E_2 or TNF-α, respectively. In the experiment to measure the concentration of Prostaglandin E_2, cells were pre-treated with indomethacin (100 μM) as a control study. Data represents box-and-whisker plots. Statistical analysis was done by a Kruskal-Wallis test (**b**, n=4;Indomethasin (+), n=7;Indomethasin (-)) or Mann-Whitney *U* test (**c**, n=10).

*; $p<0.05$. n.d.; not detectable.

Additional file 3 (xls) The list of over-expressed genes in aneurysms.

Additional file 4 (xls) The list of under-expressed genes in aneurysms.
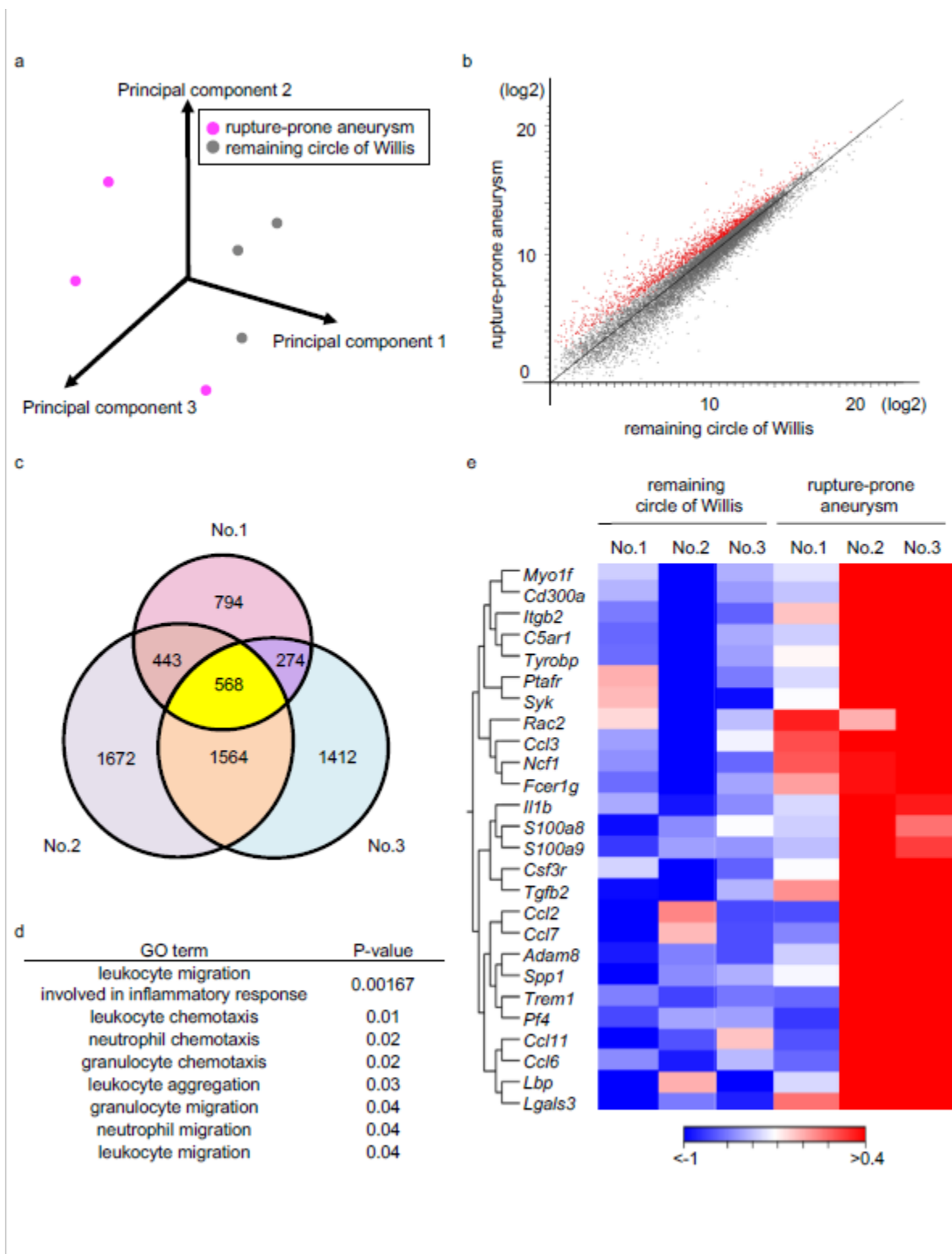
Figures

Figure 1

omprehensive gene expression profile analysis of rupture-prone IAs and the remaining circle of Willis a The principal component analysis of comprehensive gene expression profile data from rupture-prone IAs and the remaining circle of Willis (n=3). b The scatterplot showing the over-expressed genes (shown in red) in rupture-prone IAs compared to those in the remaining circle of Willis. c The Venn diagram showing the over-expressed genes in each rupture-prone lesion compared to those in the remaining circle of Willis

from a same animal (n=3). Yellow color indicates genes over-expressed in all rupture-prone lesions in common. d Identification of neutrophil-related terms in gene ontology analysis using 568 over-expressed genes. e The heat map showing gene expression profile of over-expressed genes in each rupture prone lesion and the remaining circle of Willis.
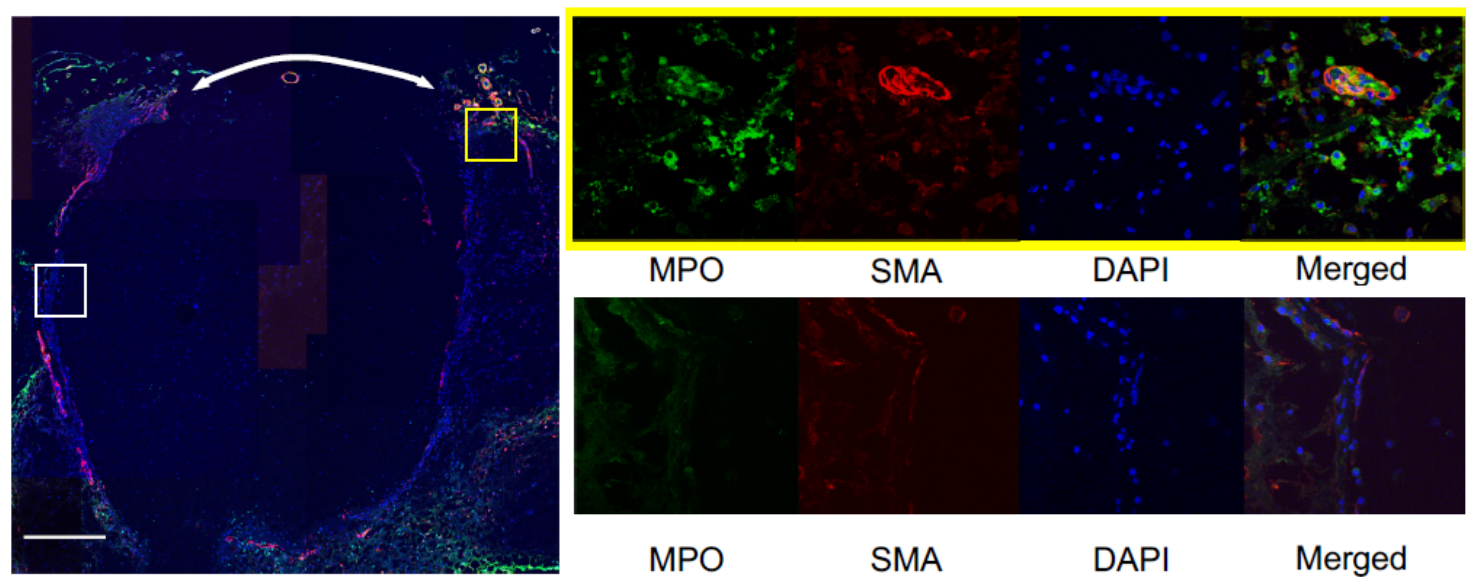

Figure 2

Accumulation of neutrophils around the site of rupture in IA lesions Abundant infiltration of myeloperoxidase (MPO)-positive cells and predominance of the presence of vasa vasorum with α-smooth muscle actin (SMA) positive media around the site of rupture. The representative images of immunostaining for MPO (green), SMA (red), of nuclear staining by DAPI (blue) and merged images are shown. The magnified images corresponding to the squares in the left panel are shown on the right. The arrows indicate the site of rupture. Bar; 100 μm.
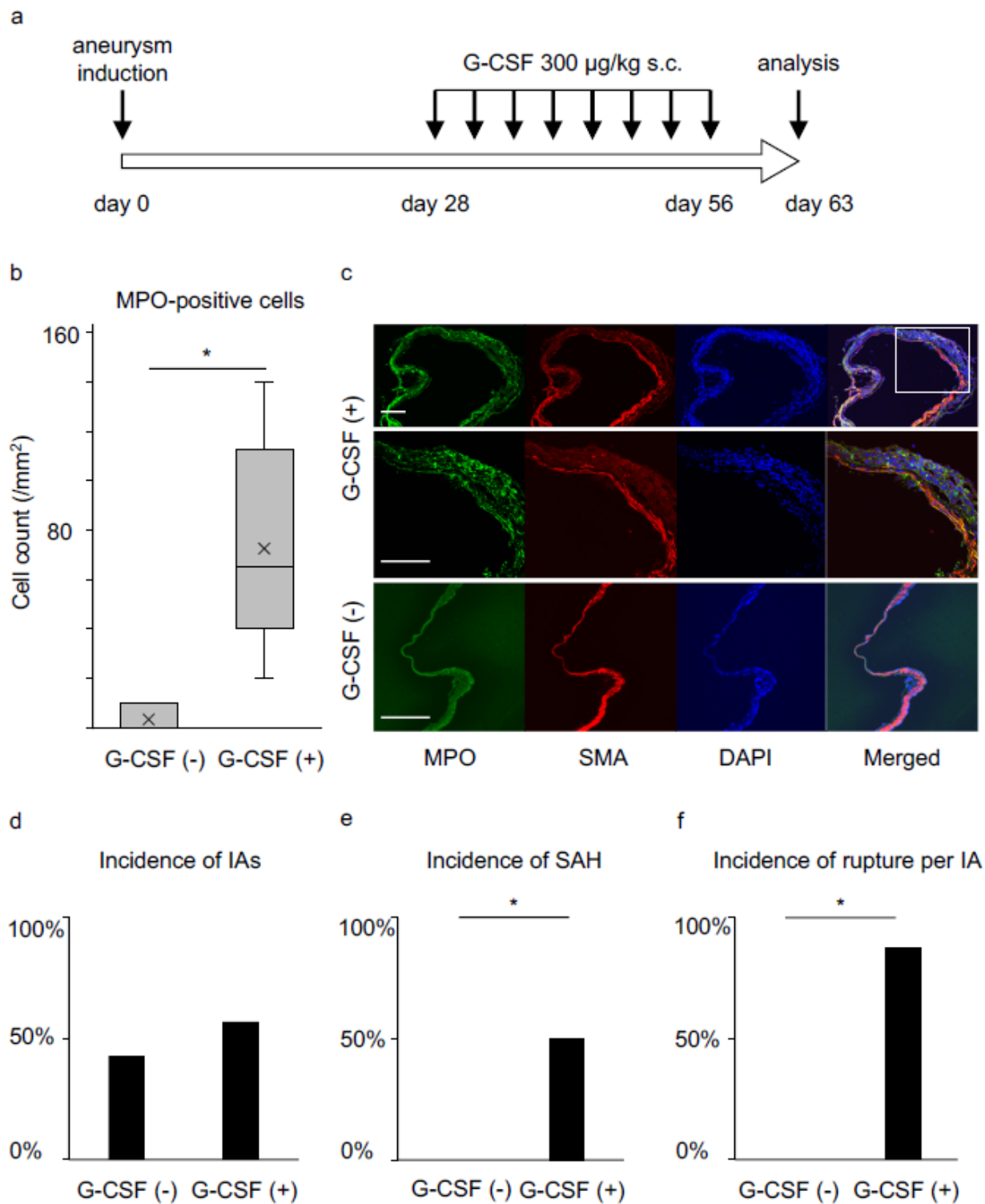
Figure 3

Administration of G-CSF and the increase in the number of neutrophils in IA lesions a Time course of the experiment. b-c Increase of myeloperoxidase (MPO)-positive cells infiltrating in IA walls of rats treated with G-CSF. IA lesions were harvested from rats subjected to an IA model and treated with G-CSF (300 μg/kg, G-CSF (+), n=14) or vehicle (G-CSF (-), n=7) and immunostained. The cell count of MPO-positive cells, neutrophils, is shown in b. Data represents box-and-whisker plots. Statistical analysis was done by

a Mann-Whitney U test. *; p<0.05. The representative images of immunostaining for MPO (green), α-smooth muscle actin (SMA, red), of nuclear staining by DAPI (blue) and merged images are shown in c. Bar; 100 μm. d-f Effect of increased neutrophils by treatment with G-CSF on incidence or rupture of IAs. Rats were subjected to IA induction and treated with G-CSF as shown in a. The incidence or rupture of IAs at the anterior- or posterior-communicating artery was examined (vehicle-treated group, n=3, G-CSF-treated group, n=8). Statistical analysis was done by a Fisher's exact test. *; p<0.05.
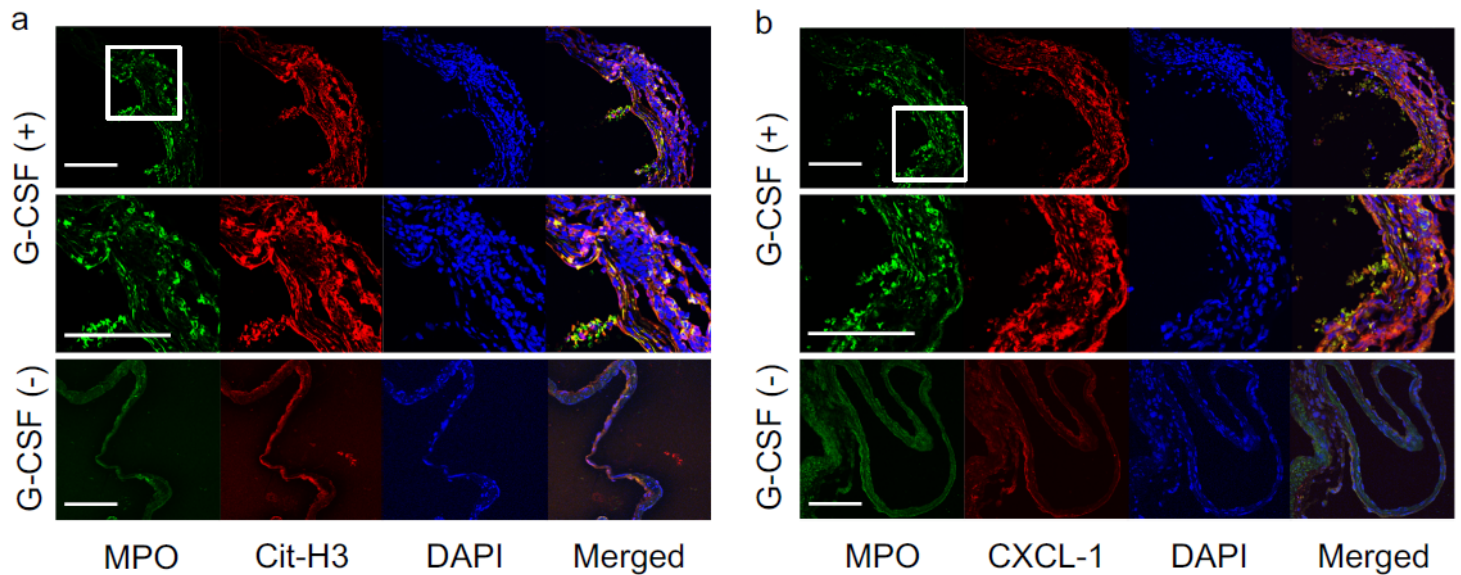

Figure 4

Activation and CXCL-1 induction in neutrophils in lesions from a rat model treated with G-CSF IA lesions were harvested from rats subjected to an IA model and treated with G-CSF (300 μg/kg, G-CSF (+)) or vehicle (G-CSF (-)) as shown in Fig. 3a and immunostained. The representative images of immunostaining for myeloperoxidase (MPO, green), citrullinated Histone H3 (Cit-H3, red in a), CXCL-1 (red in b), of nuclear staining by DAPI (blue) and merged images are shown. The magnified images corresponding to the squares in the upper panels are shown in the lower panels. Bar; 100 μm.
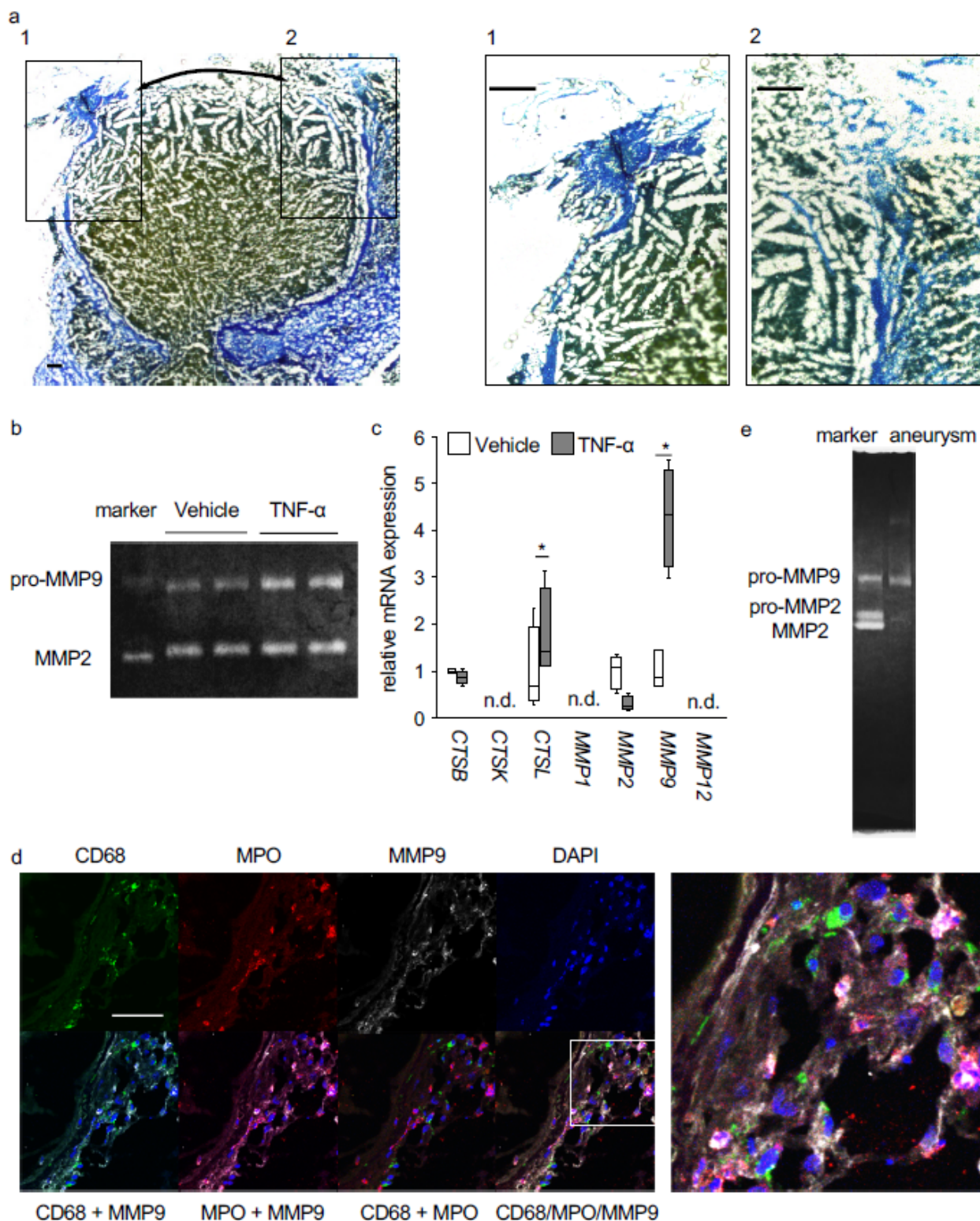
Figure 5

Production of MMP9 from neutrophils infiltrating in IA lesions a The degenerative changes of collagens around the site of rupture in IA lesions. The representative images of AZAN staining of IA lesions induced in a rat model are shown. Arrows in the left panel indicate the site of rupture. The magnified images corresponding the squares in the left panel are also shown on the right. Bar; 100 μm. b Collagenolytic activity of neutrophils. Cultured neutrophils (HL-60 cells) were stimulated with recombinant TNF-α (100

μg/ml, 5 h) and the collagenolytic activity in the supernatant was examined by a gelatin zymography using recombinant pro-MMP9, pro-MMP2 and MMP2 as a reference. The representative image of the gel from a gelatin zymography is shown. c Induction of MMP9 by TNF-α in neutrophils. Neutrophils were stimulated with recombinant TNF-α (100 μg/ml, 90 min) and the expression of proteinases was examined in RT-PCR analysis (n=4, except vehicle of MMP9; n=3). Data represents box-and-whisker plots. Statistical analysis was done by a Mann-Whitney U test. *; p<0.05. n.d.; not detectable. d Expression of MMP9 in neutrophils infiltrating in lesions. IA lesions were harvested from rats subjected to an IA model and immunostained. The representative images of immunostaining for a macrophage marker, CD68, (green), myeloperoxidase (MPO, red), MMP9 (white), of nuclear staining by DAPI (blue) and merged images are shown. The magnified image corresponding to the square is shown on the right. Bar; 50 μm. e Detection of the collagenolytic activity of MMP9 in ruptured IA lesion. Ruptured IA lesions were harvested from rats subjected to an IA model and grinded. Collagenolytic activity was then examined by a gelatin zymography using recombinant pro-MMP9, pro-MMP2 and MMP2 as a reference. The representative image of the gel from a gelatin zymography is shown.

Supplementary Files

This is a list of supplementary files associated with this preprint. Click to download.

- Additionalfile2.pdf
- Additionalfile1.xlsx
- Additionalfile3.xlsx
- Additionalfile4.xlsx